General and Comparative Endocrinology 281 (2019) 58–66

Contents lists available at ScienceDirect

General and Comparative Endocrinology

journal homepage: www.elsevier.com/locate/ygcen

Seasonal expressions of growth hormone receptor, insulin-like growth factor 1 and insulin-like growth factor 1 receptor in the scented glands of the muskrats (*Ondatra zibethicus*)

Wenqian Xie, Zeqi Tang, Yuanyuan Guo, Chunjiao Zhang, Haolin Zhang, Yingying Han, Zhengrong Yuan, Qiang Weng*

Laboratory of Animal Physiology, College of Biological Sciences and Technology, Beijing Forestry University, Beijing 100083, China

ARTICLE INFO

Keywords:
Insulin-like growth factor 1 receptor
Growth hormone receptor
MicroRNA
Muskrat
Scented gland
Seasonal changes

ABSTRACT

The growth hormone (GH)/insulin-like growth factor-1 (IGF-1) system plays an important role in regulating the cellular growth and organ development. The present study investigated the seasonal expressions of growth hormone receptor (GHR), IGF-1 and insulin-like growth factor 1 receptor (IGF-1R) in the scented glands of the muskrats. Morphological changes in the scented glands of the muskrats were observed significantly between the breeding and non-breeding seasons. Immunohistochemically, the expressions of GH, GHR, IGF-1 and IGF-1R were found in glandular cells and epithelial cells of the scented glands in both seasons. The protein and mRNA expression levels of GHR, IGF-1 and IGF-1R in the scented glands during the breeding season were noticeably higher than those of the non-breeding season. In parallel, the levels of GH and IGF-1 in the sera and scented glands were remarkably higher during the breeding season. In addition, small RNA sequencing showed that the predicted targets of the significantly changed hsa-miR-5100 and mmu-miR-6937-5p might regulate the expressions of *Ghr*, *Igf-1* or *Igf-1r*. These results suggested that the morphological changes in the scented glands of the muskrats during the different seasons might be related to the expression levels of GHR, IGF-1 and IGF-1R. Meanwhile, GHR/IGF-1 system might regulate the scented glandular functions *via* endocrine or autocrine/paracrine manners.

1. Introduction

Growth hormone (GH) is classically identified as an endocrine hormone that is synthesized and released from the anterior pituitary gland into systemic circulation and exerts pleiotropic physiological roles by regulating the growth of many target tissues in all vertebrates (Hrabia et al., 2008; Harvey et al., 2015; Ahumada-Solorzano et al., 2016). In addition to its key role in metabolism and body growth, it is known as a regulator of immunity, osmoregulation, and reproduction, which it is required for a proper control of puberty, sexual maturation, steroidogenesis and gametogenesis (Harvey and Baudet, 2014). These biological effects of GH are mediated *via* the growth hormone receptor (GHR), which is a member of the cytokine/hematopoietin receptor superfamily. GHR is a single-chain transmembrane glycoprotein, which is composed of around 620 amino acids and can be encoded by a single gene (Argetsinger and Carter-Su, 1996). Additionally, GHR is presented in the widespread organs including the reproductive and non-reproductive tissues (Hull and Harvey, 2000; Kaiser et al., 2001). Correspondingly, previous studies demonstrate that GH is also presented in many extra-pituitary tissues, in which it may act as an autocrine/paracrine growth factor (Harvey, 2010; Harvey and Baudet, 2014; Harvey et al., 2015).

Insulin-like growth factor 1 (IGF-1) is a polypeptide that acts as the major mediator of GH effects in many tissues, which is mainly produced by the liver under GH stimulus and in turn, promotes growth actions by the expression of its own receptor in many target cells (Butler and Le-Roith, 2001; Bougneres and Goffin, 2007). Besides the role as a mediator of promoting growth effects of GH, IGF-1 has an additional role in promoting growth and the maintenance of development, cellular growth, differentiation, protein translation, metabolism, apoptosis, and aging (Dantzer and Swanson, 2012). The physiological action of IGF-1 is elicited *via* insulin-like growth factor 1 receptor (IGF-1R), which is a trans-membrane tetrameric complex composed of two α and two β subunits (Leroith et al., 2008; Villalpando et al., 2008). The localization of IGF-1R was precisely described in multiple organs of some species, namely, in rat, pig, equine (Villalpando et al., 2008; Yoon et al., 2011).

* Corresponding author at: Laboratory of Animal Physiology, College of Biological Sciences and Biotechnology, Beijing Forestry University, Beijing 100083, China.
E-mail address: qiangweng@bjfu.edu.cn (Q. Weng).

https://doi.org/10.1016/j.ygcen.2019.05.014
Received 30 March 2019; Received in revised form 11 May 2019; Accepted 18 May 2019
Available online 20 May 2019

Numerous studies have shown the critical role of the GH/IGF-1 axis in directing growth and development. GHR-deficiency or IGF-1-deficiency mice had reduced body mass and tissues mass, while overexpression of GH or IGF-1 in mice increased the mass of adult mice (Lupu et al., 2001; Pitetti et al., 2013). Circulating IGF-1 in serum is derived mainly from the liver. However, liver-specific deletion of IGF-1 did not result in severe retardation of growth (Sjogren et al., 1999), which indicated that locally produced IGF-1 might promote body growth in an autocrine/paracrine manner (Hyun, 2013).

MicroRNAs (miRNAs) are endogenous ~22 nt RNAs that exert a vital role by pairing to the mRNAs of protein-coding genes to direct their posttranscriptional repression (Bartel, 2004). Previous studies have explored the regulatory mechanism of miRNAs that can simultaneously silence hundreds of target genes, and have key roles in the large-scale transcriptomic changes (Bartel, 2009; Shenoy and Blelloch, 2014). Emerging evidence suggested that miRNAs might play important roles in regulating the IGF-1 signaling. For example, deletion of miRNAs (miR-8, miR-200) resulted in defective IGF signaling and decreased body size (Jing et al., 2015). To date, several studies have investigated the expression of multiple miRNAs that mediated the GH/IGF axis on cell proliferation and differentiation (Jing et al., 2015; Lui, 2017). In our previous studies, miRNAs sequencing revealed seasonal changes in the expression profiles of miRNAs in the scented glands of the muskrats (*Ondatra zibethicus*) (Cao et al., 2015; Zhang et al., 2017b). Significantly changed miRNAs (e.g. hsa-miR-202-5p, mmu-miR-126b-5p and mmu-miR-5119) were considered to be involved in regulating the scented glands (Zhang et al., 2017a). However, the expressions and functions of most miRNAs targeting the GH/IGF-1 system in the muskrat scented gland remain unclear.

The muskrat is a medium-sized mammal that inhabits areas abundant in water like wetlands, ponds, lakes and native to North America, with a range that extends from Canada, down to northern parts of Mexico (Li et al., 2011). The name of the muskrat derives from the musky odor of secretions from paired perineal glands beneath the skin near its tail (Cao et al., 2015). The muskrat reaches sexual maturity at the age of 1 to 2 and is characterized by seasonal breeding which takes place from March to October. Reproductive seasonality results from the cyclic changes in testicular and scented glandular structure and activity, and indicates the presence of molecular mechanisms responsible for stimulation of cell proliferation and spermatogenesis induction during testis and scented glandular growth in the breeding period (Zhang et al., 2017d). The proper functioning of reproduction-related organs is controlled by an orchestra of peptide and steroid hormones (Kleinberg and Ruan, 2008; Wang et al., 2017). Our previous studies have shown that the scented gland of the muskrat was the target organ of the pituitary-derived hormones including prolactin, follicle stimulating hormone (FSH) and luteinizing hormone (LH) (Cao et al., 2015; Zhang et al., 2017c; Xie et al., 2019). Moreover, several studies suggest that the scented gland also expresses steroidogenic enzymes and is capable of sex hormone synthesis, which in turn affect the scented glandular functions *via* their receptors (Li et al., 2011; Lu et al., 2011; Lu et al., 2014; Han et al., 2017; Zhang et al., 2017a; Zhang et al., 2017b). To date, few studies have investigated the relation between GH and organs of seasonal animals. To this end, the objective of this study was to investigate the seasonal changes in the expressions of GH and IGF-1 during the breeding and non-breeding seasons in the scented glands of the muskrats, which would complement the relationship between the GH/IGF-1 and scented glandular functions in the muskrats.

2. Materials and methods

2.1. Animals

Eight adult muskrats (750–880 g body mass) were collected in December (the non-breeding season, n = 4) and May (the breeding season, n = 4) from Xinji Muskrats Breeding Farm, Hebei Province, China. The animals were paralyzed with the use of anaesthetics according to approved guidelines for the National Animal Welfare Legislation. Each pair of scented glands and testes were excised from the male muskrats after sacrifice. One side of the scented glands and testes were immediately frozen in liquid nitrogen and stored at −80 °C for RNA isolation, Western blotting and hormone assays; the others were weighted and fixed immediately for 12 h in Bouin's solution, and then stored in 70% ethanol for histological and immunohistochemical observations. Sera samples were immediately collected (6:00p.m. to 9:00p.m) and preserved in heparin-containing tubes and centrifuged at 3000 × *g* in 4 °C and the stored at −80 °C for hormonal analysis.

2.2. Histology

The scented glandular and testicular samples were dehydrated in ethanol series and embedded in paraffin wax. Serial sections (5 μm) were mounted on slides. Some sections were stained with haematoxylin and eosin following standard procedures for general histology observation. The rest of the sections were processed for immunohistochemistry.

2.3. Immunohistochemistry

Briefly, the serial sections of the scented glandular tissues were blocked with 10% normal goat serum and then incubated with primary polyclonal antibodies in 1:200 dilution against GH (bs-6579R, Biosynthesis Biotechnology, Beijing, China), GHR (bs-0654R, Biosynthesis Biotechnology, Beijing, China), IGF-1 (ab40657, Abcam, Cambridge, UK), IGF-1R (ab90657, Abcam, Cambridge, UK), Ki-67 (9449s, Cell Signaling Technology, Danvers, MA, USA) and p27 (sc-1641, Santa Cruz Biotechnology, Dallas, TX, USA) for 12 h under 4 °C. The control sections were treated with normal rabbit IgG (DE0602, Biodee Biotechnology, Beijing, China) or normal mouse IgG (DE0601, Biodee Biotechnology, Beijing, China) at 1:2000 dilutions instead of the primary antibody. The sections were then incubated with a secondary antibody, goat anti-rabbit IgG or goat anti-mouse IgG conjugated with biotin and peroxidase with avidin, using rabbit or mouse ExtrAvidin Peroxidase staining Kit (Sigma Chemical Co., St. Louis, MO, USA), followed by visualizing with 20 mg 3, 3-diaminobenzidine (Wako, Tokyo, Japan) solution in 100 ml of 0.05 M Tris–HCl buffer, pH 7.6, plus 17 μl H_2O_2. The immunostained slides were examined using a photomicroscope (BX51, Olympus, Tokyo, Japan). A semi-quantitative score for positivity (− negative, to + + + very strong positive) was analysed as described by Xie et al. (2019). The positive cell number of glandular cells stained with anti-Ki-67 or anti-p27 in the muskrat scented glands was assessed with NIH ImageJ software, with the method described by Grishagin (2015).

2.4. Reverse transcription-polymerase chain reaction (RT-PCR)

Total RNAs from each sample was extracted using TRIzol Reagent (Invitrogen Co., Carlsbad, CA, USA) in accordance with the manufacture's protocol. The total RNAs was prepared as described by Han et al. (2017). The integrity of RNA was tested by gel electrophoresis and its concentration was measured with spectrophotometer. The first-strand cDNA from total RNA was synthesized using StarScript II First-strand cDNA Synthesis Mix (GenStar, Beijing, China). The 10 μl of reaction mixture contained 1.5 μg of total RNA, 0.5 μl of Random Primer, 0.5 μl of StarScript II RT Mix, 5 μl of 2 × Reaction mix, 2.5 μl of diethylprocarbonate-ddH_2O according to the manufacturer's protocol. The PCR amplification was performed with 20 μl of reaction mixture containing 1 μl of first-strand cDNA, 1 μl each primer (10 μM), 7 μl ddH_2O, 10 μl 2 × Taq PCR StarMix with Loading Dye (GenStar, Beijing, China) under the following condition: 94 °C for 2 min for the initial denaturation of the cDNA hybrid, 35 cycles of 94 °C for 30 sec, 58 °C for 30 s and 72 °C for 30 sec with a final extension of 5 min at 72 °C. The cDNA

fragment was amplified by *Ghr*-F: 5′-TCACCACAGAAAGCCTTACC-3′ and R: 5′-TTCAGTTGGTCTGTGCTCAC-3′; *Igf-1*-F: 5′-CTTCAGTTCGTG TGTGGACC-3′ and R: 5′-GTCTTGGGCATGTCAGTGTG-3′; *Igf-1r*-F: 5′-CGATATCCACAGCTGCAACC-3′ and R: 5′-GACACACATTCCCGCTG ATC-3′. The PCR products were electrophoresed in the 1% agarose gel and individual bands visualized by GelRed (Biotium Inc., Fremont, CA, USA) staining. The gene *Actb* was selected as the endogenous control. The optical absorbance density was measured by ImageJ, and the relative density of target gene was normalized to that of *Actb*. DNA sequence samples were sent to Omega Genetics Co., Ltd (Beijing, China), and determined using the ABIPRISM 3730 sequencer (Invitrogen Co., Carlsbad, CA, USA). After obtaining the sequence of each PCR product, it was blasted with known mRNA sequence for rat, mouse, bovine and human, found the homologous sequence fragment in each species and compared for homology.

2.5. Quantitative real-time PCR

The cDNA was stored at −20 °C. The cDNA fragment used for quantitative real-time PCR was amplified by primers *Gh*-F: 5′-GTTCG AGCGTGCCTACATTC-3′ and R: 5′-TTCTCATAGACGCGGTCCGA-3′; *Ghr*-F: 5′-CAACTGCTTTGCCTTTGCCT-3′ and R: 5′-TCCACTCTCATGCT CTCCCA-3′; *Igf-1*-F: 5′-CTGGTGGACGCTCTTCAGTT-3′ and R: 5′-CTTC AGCGGAGCACAGTACA-3′; *Igf-1r*-F: 5′-CCCAACTCTGCCCAATGGTA-3′ and R: 5′-CGGCGTACTTTCTGATGGGT-3′. The annealing temperature used for all primers was 60 °C. The PCR reactions were carried out in a 10 μl volume using FastStart Essential DNA Green Master (Roche Molecular System Inc., Basel, Switzerland). The PCR conditions were performed in ABI PRISM 7500 Fast Real-Time System (Applied Biosystems, Foster City, CA, USA) as described below: 10 min at 95 °C, followed by 40 cycles of 30 s at 95 °C, 30 s at 60 °C and 30 s at 72 °C. The melting curves were also performed to test the homogeneity of the PCR products by increasing the temperature progressively to 95 °C, then decreasing it to 65 °C for 60 sec and increasing it again to 95 °C. The target and reference genes had the similar PCR efficiency. Negative control reactions in the absence of reverse transcriptase were performed to test for genomic DNA contamination. All samples were run in triplicate, including a negative control and the intra-assay variation was less than 10%. The expression level of each target mRNA relative to *Actb* mRNA was determined using the $2^{-\Delta\Delta Ct}$ method.

2.6. Protein isolation and Western blotting analysis

Tissues were homogenized using high-speed homogenizer (Bead Ruptor12, OMNI International Co., Ltd., CA, USA) in PBS. The total homogenate was centrifuged at 12,000 × *g* for 6 min at 4 °C. Protein extracts (30 μg) were mixed with an equal volume of 2 × Laemmli sample buffer. Equal amounts of each sample were loaded and run on a 12% SDS-PAGE gel at 18 V/cm and transferred to PVDF membranes using a wet trans-blotting apparatus (Bio-Rad, Richmond, CA, USA). The membranes were blocked in 3% bovine serum albumin (BSA) for 1 h at room temperature and incubated overnight in one of the primary antibodies: rabbit polyclonal anti-GHR (1:500 dilution), rabbit polyclonal anti-IGF1 (1:1000 dilution), rabbit polyclonal anti-IGF1R (1:1000 dilution), mouse polyclonal anti-Vinculin (1:1000 dilution) (sc-73614, Santa Cruz Biotechnology, CA, USA) or mouse polyclonal anti-β-actin (1:1000 dilution) (AM1021B, Abgent Biotechnology, Suzhou, China) prepared in 1% BSA in Tris-buffered saline (TBS)-0.05% Tween 20. Secondary incubation of the membrane used a 1:5000 dilution of goat anti-rabbit IgG tagged or goat anti-mouse IgG with horseradish peroxidase for 1 h at room temperature. Finally, Proteins were visualized using an enhanced chemiluminescence (ECL) kit and protein content was determined by scanning exposed X-ray film.

2.7. Hormone measurement

The scented gland and serum samples from each animal were analysed by the enzyme linked immunosorbent assay (ELISA) to detect GH and IGF-1 concentrations using the ELISA Kit (Kit CSB-E07342r for GH and Kit CSB-E04582r for IGF-1, Cusabio Biotech Co., Ltd., Wuhan, China). Briefly, 100 μl per well of tissue samples, sera samples or standard were added into the assay plate which were coated with goat-anti-rabbit IgG antibody. The microplate was covered with a new adhesive strip and incubated for 2 h at 37 °C, and then remove the liquid of each well. 100 μl of biotin-antibody were added to each well of the plate and then incubated for 1 h at 37 °C. After aspirating and washing 3 times with 200 μl wash buffer, 100 μl per well of HRP-avidin were added into the plate and incubated for 1 h at 37 °C. After aspirating and washing 5 times with 200 μl wash buffer, the assay plate was colored and read using a microplate reader (PT 3502G, Beijing Potenov Technology Co., Ltd., Beijing, China) at 450 nm within 10 min. The detection limitation for GH and IGF-1 Kit is 0.78 pg/ml and 0.15 ng/ml, respectively. The validation of ELISA Kit for muskrats were checked by examining the parallelism between the standard curve and series diluted sample curve (Fig. S1a, b). The intra- and inter-assay coefficient of variation were 1.01% and 4.47% in the assay using GH Kit and 3.28% and 6.89% in the assay using IGF-1 Kit, respectively.

2.8. MicroRNAs-sequencing and bioinformatic analysis

The miRNA sequencing and analysis were previously described in detail (Cao et al., 2015). Briefly, the small RNA (sRNA) libraries for the scented gland of muskrat from the breeding season (named: SGB1) and the non-breeding season (named: SGNB2) were constructed from total RNAs using the Illumina Truseq Small RNA Preparation Kit (RS-930-1012, Illumina Inc., San Diego, CA, USA), and were sequenced on the Illumina GAIIx platform following the vendor s recommended protocol at Beijing Yuanquanyike Biological Technology Co., Ltd (Beijing, China). The target genes regulated by miRNAs were predicted using the miRanda (version 3.3a, http://www.microrna.org/microrna/) and Target Scan Human (version 7.0, http://www.targetscan.org/vert_70/). R software was utilized to analyze the correlation between differential expression profile of miRNAs and their targeted genes.

2.9. Statistical analysis

Statistical analyses were made with the Student's *t*-test and performed on GraphPad Prism 7.0 (GraphPad Software Inc., CA, USA). Data were given as means ± SEM. $P < 0.05$ was considered statistically significant.

3. Results

3.1. Morphological and histological observation in the muskrat

Morphological and histological observations of the muskrat scented glands and testes were presented in the male muskrat (Fig. 1). The scented glands, located in the ventral base of the tail between the skin and muscle layer, were situated anatomically inferior to the testis and epididymis (Fig. 1a). The significant reduction of the morphological size of the scented gland and the testis in the non-breeding season was found when comparing to the breeding season (Fig. 1b). Histological structure of the scented glands and testes in the male muskrats by haematoxylin-eosin (HE) were set out (Fig. 1c). A cross section of the muskrat testes between the periods of breeding and non-breeding revealed the differences, and that all types of germ cells were shown in the muskrat testes of the breeding season, while only spermatogonia and primary spermatocytes could be identified in the non-breeding season (Fig. 1c-i, ii). The differences of testicular cells indicated the reproductive status of the muskrats during the seasonal changes. The

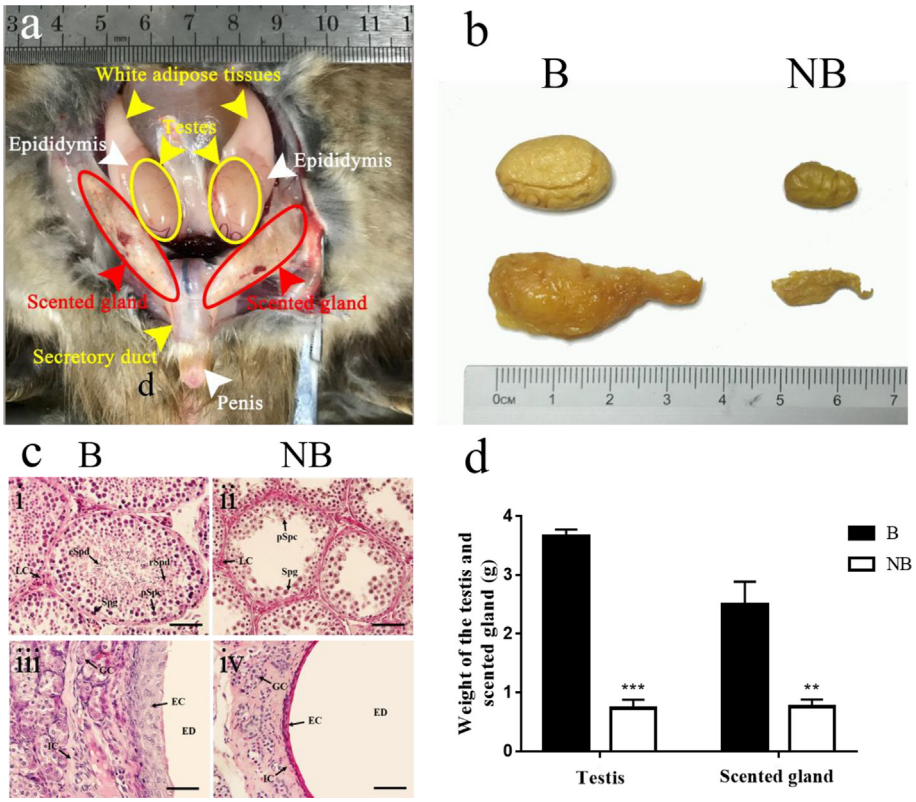

Fig. 1. Anatomic localization and morphology of the muskrat scented glands and testes. The anatomic localization and morphology of the scented glands and testes (a). The morphology of the scented glands after fixation during the breeding and non-breeding seasons (b). Histological structure of the muskrats scented glands and testes by hematoxylin-eosin (HE) (c). Histological observation of the testes in the breeding (i) and the non-breeding seasons (ii). Histological observations of the scented glands in the breeding (iii) and the non-breeding seasons (iv). The average weight of the scented glands and testes in the breeding and non-breeding seasons (d). ED, excretory duct; GC, glandular cell; EC, epithelial cell; IC, interstitial cell; LC, Leydig cells; SC, Sertoli cells; Spg, spermatogonia; pSpc, primary spermatocytes; rSpd, round spermatids; eSpd, elongate spermatids; B, the breeding season; NB, the non-breeding season; Scale bars represent 50 μm. The error bars represent means ± SEM (n = 6, each period). *Statistically significant values (**$P < 0.01$; ***$P < 0.001$).

three types of cells, including epithelial cells, glandular cells and interstitial cells were observed in the scented glands during both seasons (Fig. 1c-iii, iv). In addition, the average weight of scented glands and testes in the breeding season showed conspicuously higher ($P < 0.01$ and $P < 0.001$) than those of the non-breeding season (Fig. 1d).

3.2. Immunohistochemical localizations of GH, GHR, IGF-1, IGF-1R, Ki-67 and p27 in the scented glandular cells of the muskrats

Immunolocalizations of GH, GHR, IGF-1 and IGF-1R in the scented glands of the muskrats during the breeding and non-breeding seasons were presented in Fig. 2. The immunoreactivity of GH and GHR was detected in the cytoplasm of epithelial cells and glandular cells, but not in interstitial cells, in both seasons (Fig. 2a-h). The positive signals of IGF-1 and IGF-1R were localized at the cytoplasm of the glandular cells and epithelial cells in the breeding season (Fig. 2i, j, m, n). Notably, the staining signal was only weakly detected in the cytoplasm of the epithelial cells and glandular cells in the non-breeding season, whereas no signal observed in the interstitial cells (Fig. 2k, l, o, p, Table 1). There was no staining observed in the negative control group (Fig. 2q–t).

To assess cell proliferation in the scented gland during the breeding and non-breeding seasons, the immunolocalizations of Ki-67 and p27, as the marker of cell proliferation and cell cycle inhibitor, were examined and the results were presented in Fig. 3. Ki-67 was localized in nuclei of glandular cells and epithelial cells in the breeding season, however, it was weakly ($P < 0.001$) detected in those cells during the non-breeding season (Fig. 3a, b, d, e, Tables 1 and 2). On the other side, p27 was immunolocalized in the nuclei of glandular cells and epithelial cells, but not in interstitial cells during both seasons. The positive signal of p27 in glandular cells and epithelial cells in the non-breeding season was higher ($P < 0.001$) than those of the breeding season (Fig. 3g, h, j, k, Tables 1 and 2). No signal was observed in the negative control group (Fig. 3c, f, i, l). The staining results obtained from the images were quantified and summarized in Table 1. The proportion of positive glandular cells for Ki-67 and p27 staining results were summarized in Table 2.

3.3. Gene expressions of Gh, Ghr, Igf-1 and Igf-1r in the scented glands of the muskrats and homologous sequence comparison

The relative mRNA expression levels of *Gh*, *Ghr*, *Igf-1* and *Igf-1r* were compared between the breeding and non-breeding seasons by quantitative real-time PCR (Fig. 4a–c). The level of *Gh* and *Ghr* transcripts in the scented glands of muskrats decreased ($P < 0.01$, $P < 0.05$) notably from the breeding season to the non-breeding season (Fig. 4a, b). Similarly, the expression of *Igf-1* and *Igf-1r* was significantly higher ($P < 0.01$) in the scented glands of the breeding season, and markedly reduced in the scented glands of the non-breeding season (Fig. 4c, d). The *Ghr*, *Igf-1* and *Igf-1r* cDNA nucleotide sequence in the muskrats had high identity to those in rats (90%, 94%, 89%, respectively), mice (90%, 93%, 88%, respectively), humans (82%, 89%, 85%, respectively) and bovine (78%, 84%, 86%, respectively).

3.4. Protein expressions of GHR, IGF-1 and IGF-1R in the scented glands of the muskrats

The Western blot analysis of the protein levels of GHR, IGF-1, IGF-1R in the scented glands during the breeding and non-breeding seasons were shown in Fig. 5. The major bands for GHR, IGF-1 and IGF-1R were detected at a molecular weight of about 65 kDa, 21 kDa and 200 kDa, respectively. The relative optional density of GHR, IGF-1 and IGF-1R in the scented glands were significantly higher ($P < 0.001$ and $P < 0.05$) in the breeding season than those of the non-breeding season (Fig. 5a–c).

3.5. The concentration of GH and IGF-1 in the scented glands and sera

The concentrations of GH and IGF-1 in the scented glands and sera of the muskrats were measured by ELISA (Fig. 6). The serum GH and IGF-1 levels in the muskrats decreased ($P < 0.001$ and $P < 0.01$) from

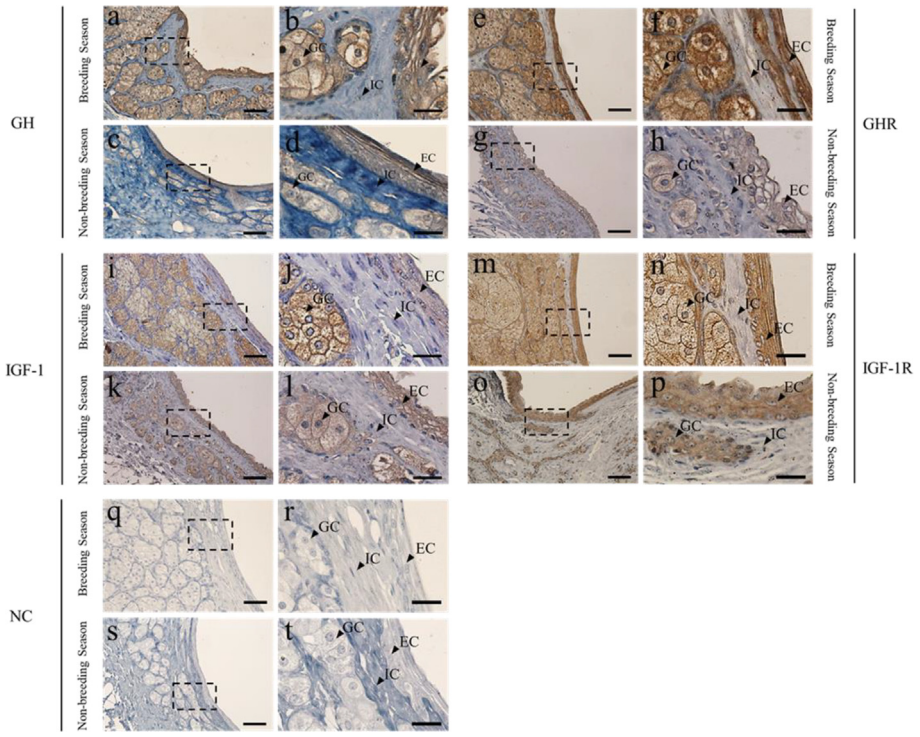

Fig. 2. Immunolocalization of GH, GHR, IGF-1 and IGF-1R in the scented glandular cells of the muskrats during the breeding and non-breeding seasons. Black arrow heads indicate the three cell types: glandular cells, epithelial cells and interstitial cells. Immunolocalization of GH in the scented glands of the breeding (a, b) and non-breeding seasons (c, d). Immunolocalization of GHR in the scented glands of the breeding (e, f) and non-breeding seasons (g, h). Immunolocalization of IGF-1 in the scented glands of the breeding (i, j) and non-breeding seasons (k, l). Immunolocalization of IGF-1R in the scented glands of the breeding (m, n) and non-breeding seasons (o, p). The negative control of the scented glands of the breeding (q, r) and non-breeding seasons (s, t). NC, negative control; GC, glandular cell; EC, epithelial cell; IC, interstitial cell. Scale bars respectively represent 25 μm (the first and third columns of pictures: a, c, e, g, i, k, m, o, q and s) and 10 μm (the second and fourth columns of pictures: b, d, f, h, j, l, n, p, r and t).

Table 1
Immunohistochemical localizations of GHR, IGF-1, IGF-1R, Ki-67 and p27 in the scented glands of the muskrats during the breeding and non-breeding seasons.[1]

	EC		GC		IC	
Antibodies	B	NB	B	NB	B	NB
GH	+ + +	+	+ + +	+	–	–
GHR	+ + +	+	+ + +	+	–	–
IGF-1	+ + +	+	+ + +	+	–	–
IGF-1R	+ + +	+	+ + +	+	–	–
Ki-67	+ + +	+	+ + +	+	–	–
p27	+ +	+ + +	+ +	+ + +	–	–

EC, epithelial cells; GC, glandular cell; IC, interstitial cells; B, the breeding season; NB, the non-breeding season.

[1] –, negative staining; +, positive staining; + +, strong positive staining; + + +, very strong positive staining.

33.42 ± 4.04 pg/ml and 2.23 ± 0.53 ng/ml in the breeding season to 3.69 ± 0.31 pg/ml and 0.16 ± 0.03 ng/ml in the non-breeding season, respectively (Fig. 6a, c). Similarly, in the scented glands, the GH and IGF-1 levels were significantly lower ($P < 0.001$) in the non-breeding season (13.49 ± 1.42 pg/g, 2.24 ± 0.03 ng/g, respectively) compared to those in the breeding season (53.81 ± 2.40 pg/g, 10.28 ± 0.34 ng/g, respectively) (Fig. 6b, d).

3.6. The bioinformatics analysis of miRNAs in the scented glands of the muskrats

The seasonal expressions of global miRNAs in this tissue were reported previously (Cao et al., 2015). To search for the miRNAs that may have a direct impact on the GH, IGF-1 and their receptors, we used two different software packages, miRanda and TargetScanHuman, to predict their target genes based on the sequences of these miRNAs and the known mRNAs. Notably, totally 15 differential expressed miRNAs were found to target *Gh*, *Ghr*, *Igf-1* and *Igf-1r*, which were shown in Table 3. In details, 5 down-regulated miRNAs including hsa-miR-5100, mmu-miR-6937-5p, has-miR-4454, mmu-miR-8112 and rno-miR-451-5p in the scented glands of the breeding season targeting to *Ghr*, *Igf-1* or *Igf-1r* were specially focused due to the expression patterns of those genes and miRNA functions, although there were the other 10 up-regulated miRNAs (Table 3). Furthermore, has-miR-5100 was predicated to target both *Ghr* and *Igf-1*, and mmu-miR-6937-5p was predicted to target both *Ghr* and *Igf-1r* (Table 3).

4. Discussion

In this study, we investigated the expressions and distribution patterns of GH, IGF-1 and IGF-1R in the scented glands of the muskrats during the breeding and non-breeding seasons. The results demonstrated that expression levels of GH, GHR, IGF-1 and IGF-1R in the scented glands of the muskrats were higher during the breeding season and then decreased significantly in the non-breeding season. In parallel, the concentration of GH and IGF-1 in the scented glands and sera were also markedly higher during the breeding season than in the non-breeding season. These findings suggested that GH and IGF-1 might be involved in the morphological and functional changes of the scented glands during different seasons.

In this study, the scented glandular size and weight were higher in the breeding season compared with the non-breeding season. The seasonality of the scented glandular size and weight of the muskrats were correlated with the histological changes of the scented glands, consistent with our previous observation (Han et al., 2017). The changes in the positive cell proportion for Ki-67 and p27 in the glandular cells of the scented glands during different seasons suggested that cell proliferative rate was higher in the breading season than that in the non-breeding season, resulting in larger size and higher weight of the scented glands. Increasing evidence showed that growth factors (e.g. GH, IGF-1) were the key regulators promoting the development and the morphogenesis of various tissues, including muscle, skin, bone, and nervous system (Sanders and Harvey, 2004). Moreover, the previous reports demonstrated that GH played a key role in the organ regression and regrowth in some seasonal breeders, such as roe deer (*Capreolus capreolus*) (Wagener et al., 2000), white-tailed deer (*Odocoileus virginianus*) (Bubenik et al., 1975) and domestic nutria (*Myocastor coypus*) (Sirotkin et al., 2003). In this study, the immunolocalization of GHR

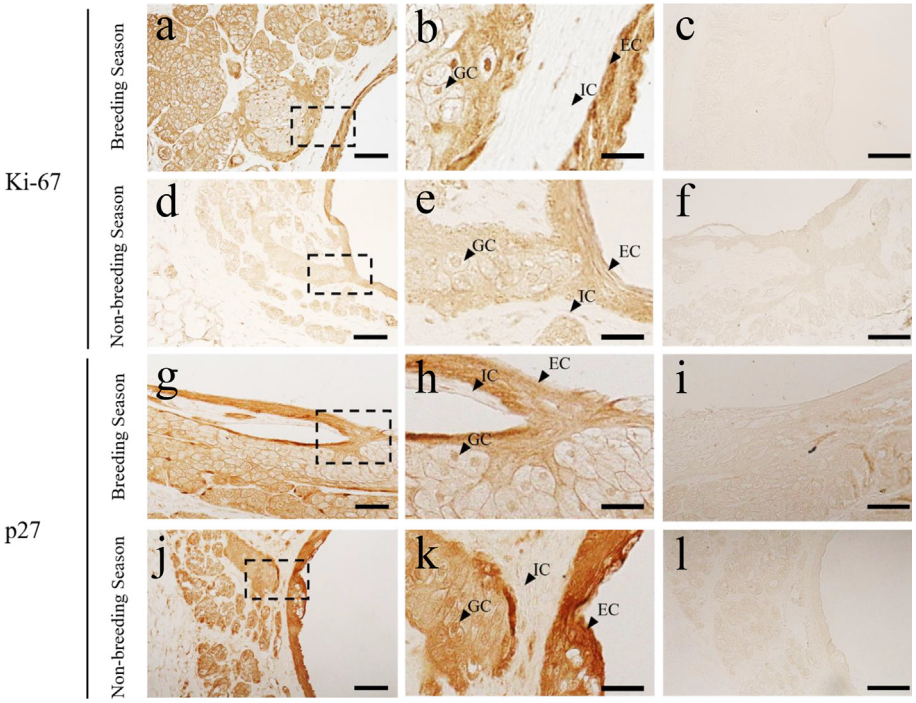

Fig. 3. Immunolocalization of Ki-67 and p27 in the scented glandular cells of the muskrats during the breeding and non-breeding seasons. Black arrow heads indicate the three cell types: glandular cells, epithelial cells and interstitial cells. Immunolocalization of Ki-67 in the scented glands of the breeding (a, b) and non-breeding seasons (d, e). Immunolocalization of p27 in the scented glands of the breeding (g, h) and non-breeding seasons (j, k). The negative control of the scented gland in the breeding (c, i) and non-breeding seasons (f, l). GC, glandular cell; EC, epithelial cell; IC, interstitial cell. Scale bars respectively represent 25 μm (the first and third columns of pictures: a, c, d, f, g, i, j, l) and 10 μm (the second columns of pictures: b, e, h, k).

Table 2
The proportion of positivity expressed nuclei in glandular cells of the scented gland of the muskrats during the breeding and non-breeding seasons.

	Proportion of positivity expressed nuclei (%)	
Antibodies	Breeding season	Non-breeding season
Ki-67	65.82 ± 0.22[a]	23.96 ± 2.20[b]
p27	35.53 ± 1.68[b]	66.69 ± 1.03[a]

[a,b]Values within a row with different superscripts differ significantly at $P < 0.001$.

showed that the glandular cells and epithelial cells were the target cells of GH in the scented glands. Furthermore, the seasonal expressions of GH levels in the scented glands and sera as well as that of GHR was in parallel with the morphological and cellular changes in the scented glands. These findings suggested that GH might be related to the morphological changes of the scented glands and promote cell proliferation.

Accumulating evidence indicated that GH might be involved in the regulation of the extra-pituitary organs *via* binding to its receptor and the induction of IGF-1 production (Harvey, 2010; Harvey and Baudet, 2014; Devesa et al., 2016). GH was previously shown to stimulate *IGF-1* gene expression to regulate the organic growth of several species (Woelfle et al., 2003). For instance, GH was able to induce IGF-1 expression in the ovarian granulosa cells in pigs and rats (Ptak et al., 2004; Nakamura et al., 2012). In the present study, the positive signals of IGF-1 and GHR were both observed in the scented glandular cells. In addition, gene expression or circulating/local IGF-1 concentrations during the different seasons had the similar trend as the circulating/local concentrations of GH. Taken together, these data suggested that

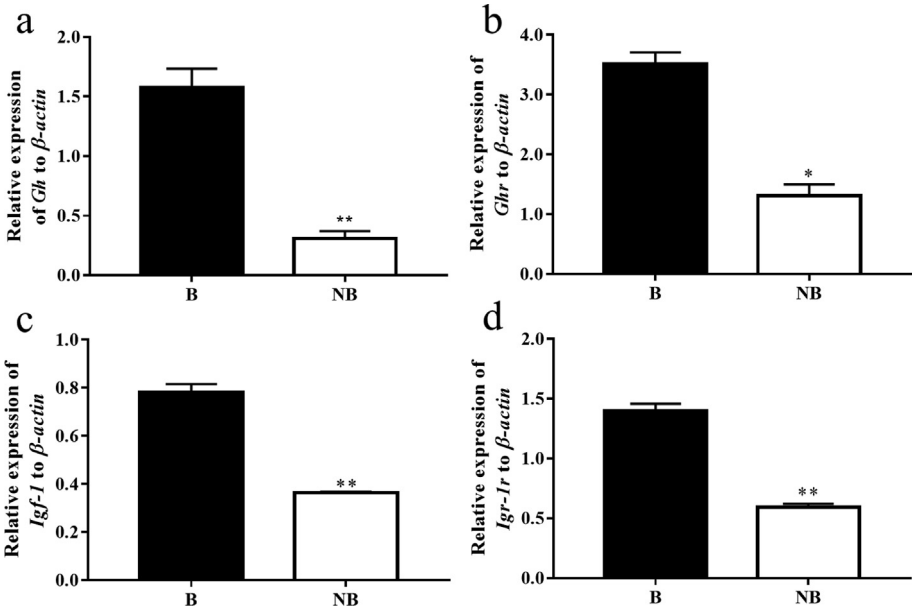

Fig. 4. Real-time PCR analysis of gene expression levels of *Gh*, *Ghr*, *Igf-1* and *Igf-1r* in the scented glands during the breeding and non-breeding seasons. The seasonal profiles of mRNA expression of *Gh* (a), *Ghr* (b), *Igf-1* (c) and *Igf-1r* (d) in the scented glands. The error bars represent means ± SEM (n = 3, each period). B, the breeding season; NB, the non-breeding season. *Statistically significant values (*$P < 0.05$, **$P < 0.01$, ***$P < 0.001$).

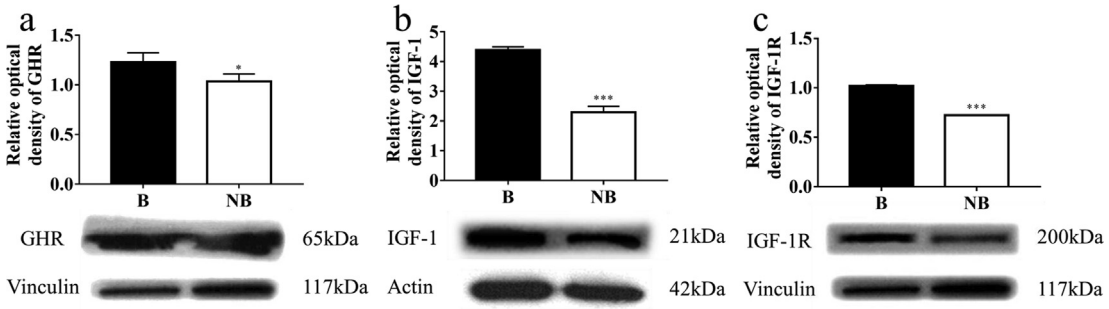

Fig. 5. Western blot analysis of the protein levels of GHR, IGF-1 and IGF-1R in the scented glands during the breeding and non-breeding seasons. The seasonal profiles of protein expression of GHR (a), IGF-1 (b) and IGF-1R (c) in the scented glands. The error bars represent means ± SEM (n = 3, each period). B, the breeding season; NB, the non-breeding season. *Statistically significant values ($^{*}P < 0.05$, $^{**}P < 0.01$, $^{***}P < 0.001$).

IGF-1 might serve as one the mediator of GH/GHR signaling pathway in the scented glandular cells. Several reports showed that IGF-1 could regulate tissue growth in mammals. For example, in the red deer, the co-existence of IGF-1 and IGF-1R in chondrocytes implied an autocrine/paracrine role in stimulating the growth of antlers (Gu et al., 2007). In rats and equine, IGF-1 and IGF-1R were localized in spermatogenic and Leydig cells, suggesting that IGF-1 may be involved in male spermatogenesis and Leydig cell functions as an autocrine/paracrine factor (Yagci and Zik, 2006; Yoon et al., 2011). Here, the mRNA and protein levels of IGF-1 were observed in the scented glands, indicating that the scented glands had the capability to locally produce IGF-1. Furthermore, the localizations of IGF-1R in the scented glandular cells were also observed, suggesting that the produced IGF-1 under the stimulation of GH/GHR signaling might act as an autocrine/paracrine factor to regulate the scented glandular functions *via* its receptor.

In mammals, organ morphogenesis is an intricate physiological process tightly regulated by a cascade network of various signaling pathways (Silberstein, 2015). Besides, previous studies have demonstrated the presence of gonadotropins receptors and steroid hormone receptors as well as the local production of steroid hormones, suggesting that gonadotropins might modulate local steroidogenesis, and the locally produced steroid hormones may affect the functions of the scented glands (Cao et al., 2015; Zhang et al., 2017a; Zhang et al., 2017c; Xie et al., 2019). Although the relationship between GH/IGF-1 signaling and other peptide or steroid hormones signaling were not investigated here, recent studies provided some clues. For instance, there were combined effects of PRL, GH and LH in Leydig cell of rats to maintenance of testicular LHR expression. Furthermore, GH-stimulated IGF-1 regulated steroidogenesis in the immature testis by inducing the expressions of steroidogenic enzymes in Leydig cells (Villalpando and López-Olmos, 2003; Berensztein et al., 2008). GH could exert combined effects with steroid hormones, such as 17β-estradiol (E_2), and stimulate the entire process of ductal morphogenesis in mammary cells dependent or independent on IGF-1 production (Kleinberg and Ruan, 2008). Together, these results shed light into the complex gene network involved in the regulation of morphological and functional changes in the scented glands of the muskrats, where steroid and peptide hormones (such as GH/IGF-1) might be involved.

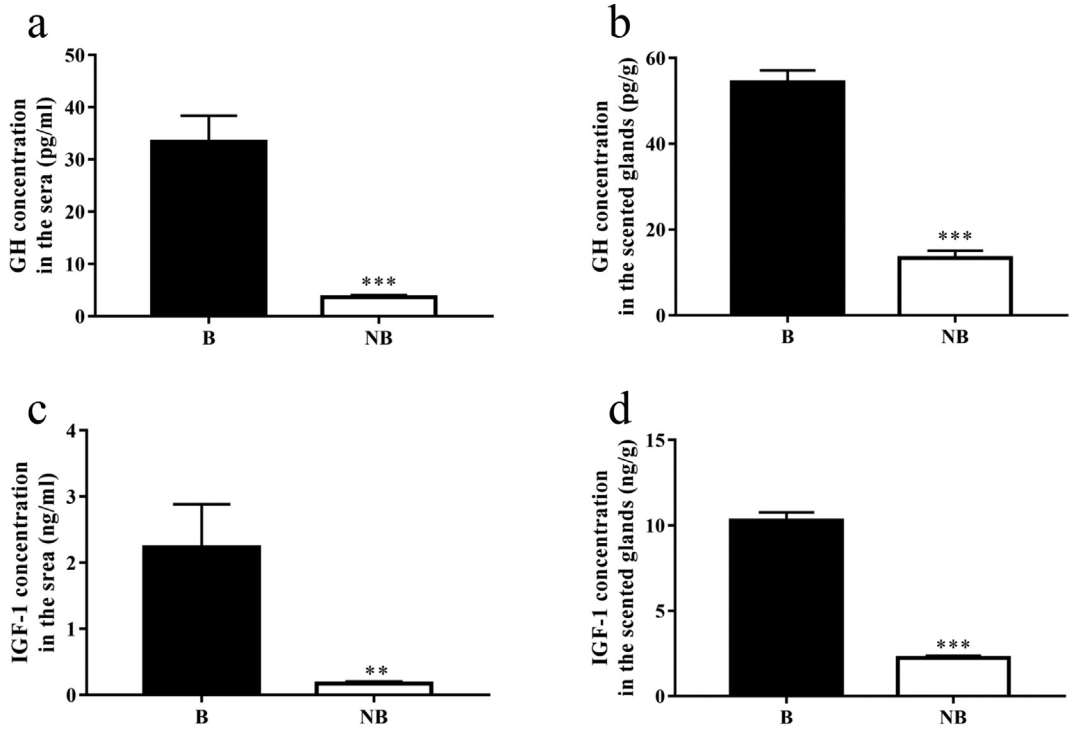

Fig. 6. The seasonal concentrations of GH and IGF-1 in the scented glands and sera during the breeding and non-breeding seasons. The concentrations of GH in the sera (a) and scented glands (b) of the muskrats. The concentrations of IGF-1 in the sera (c) and scented glands (d) of the muskrats. The error bars represent means ± SEM (n = 3, each period). B, the breeding season; NB, the non-breeding season. *Statistically significant values ($^{*}P < 0.05$, $^{**}P < 0.01$, $^{***}P < 0.001$).

Table 3
Differentially expressed miRNAs targeting *Gh*, *Ghr*, *Igf-1* and *Igf-1r*.

miRNA-Targeted *Gh*	miRNA-Targeted *Ghr*	miRNA-Targeted *Igf-1*	miRNA-Targeted *Igf-1r*
mmu-miR-126b-5p[a]	hsa-miR-1[a] hsa-miR-762[a,b] hsa-miR-5100[a]↓ mmu-miR-1b-5p[a] mmu-miR-126b-5p[a,b] mmu-miR-6937-5p[a,b] ↓ rno-miR-144-3p[b]	hsa-miR-1[a,b] hsa-miR-762[a] hsa-miR-5100[b] ↓ mmu-miR-1b-5p[a,b] mmu-miR-126b-5p[a,b] mmu-miR-5119[a] mmu-miR-7085-3p[b] rno-miR-144-5p[a] rno-miR-451-5p[b]	hsa-miR-1[b] hsa-miR-762[a,b] hsa-miR-4454[b] ↓ hsa-miR-4485[a,b] mmu-miR-1b-5p[b] mmu-miR-126b-5p[a,b] mmu-miR-5119[a,b] mmu-miR-6937-5p[b] ↓ mmu-miR-8112[a,b] ↓ rno-miR-144-3p[b] rno-miR-144-5p[b] rno-miR-147[b]↓ rno-miR-451-5p[b]

[1]↓ indicates down-regulated miRNA.
[a] miRNA targets predicted by TargetScanHuman.
[b] miRNA targets predicted by miRanda.

MiRNAs as short non-coding RNAs participate in multiple physiological functions in different types of cells (Shenoy and Blelloch, 2014). Recent studies unveiled that miRNAs can regulate the GH/IGF-1 axis and affect organ and body growth (Lui, 2017). In mice, down-regulation of growth-promoting genes (such as *Igf-1*) might be modulated by miR-29 family in multiple organs (Kamran et al., 2015). Recent evidence showed that miRNA-5100 could regulate the expression of cell proliferation factors including cyclin D1 and cyclin-dependent kinases 2 (CDK2) (Huang et al., 2015). In this study, among the 15 significantly expressed miRNAs targeting *Gh*, *Ghr*, *Igf-1* and *Igf-1r*, we focused on the 5 down-regulated miRNAs due to their opposite expression profiles to their target genes. In particular, hsa-miR-5100 and mmu-miR-6937-5p were predicted to target *Ghr* and *Igf-1* or *Igf-1r* genes, suggesting that hsa-miR-5100 and mmu-miR-6937-5p might be involved in the GH/IGF-1 signaling pathway to regulate cell proliferation of the scented glands. However, the underpinning molecular mechanism requires further validation and investigation.

5. Conclusions

In summary, the present study profiled the seasonal expressions of GH/IGF-1 and their receptors as well as the putative regulatory miRNA in the scented glands of the muskrats. These results suggested that the scented gland was likely a target of GH and IGF-1, and GH/IGF-1 system that may function in an endocrine or autocrine/paracrine manner. This study provided new insight into the functions of GH/IGF-1 in the scented glands, a non-classical endocrine organ.

Authors' contributions

WX, ZT, YG and CZ participated in sample collection, performing the experiments, analyzing the data and drafting the manuscript. HZ, YH and QW assisted with all experiments and helped revising the manuscript. YH, ZY and QW designed, supervised the study, and revised manuscript. All authors read and approved the final version.

Declaration of Competing Interest

The authors declare that they have no competing interests.

Acknowledgements

This research work was supported by National Natural Science Foundation of China (31872320, 21806010) and Natural Science Foundation of Beijing Municipal (8182039) and Young Scientist Start-up Funding of Beijing Forestry University (BLX201714).

Appendix A. Supplementary data

Supplementary data to this article can be found online at https://doi.org/10.1016/j.ygcen.2019.05.014.

References

Ahumada-Solorzano, S.M., Martinez-Moreno, C.G., Carranza, M., Avila-Mendoza, J., Luna-Acosta, J.L., Harvey, S., Luna, M., Aramburo, C., 2016. Autocrine/paracrine proliferative effect of ovarian GH and IGF-I in chicken granulosa cell cultures. Gen. Comp. Endocrinol. 234, 47–56.
Argetsinger, L.S., Carter-Su, C., 1996. Mechanism of signaling by growth hormone receptor. Physiol. Rev. 76, 1089–1107.
Bartel, D.P., 2004. MicroRNAs: genomics, biogenesis, mechanism, and function. Cell 116, 281–291.
Bartel, D.P., 2009. MicroRNAs: target recognition and regulatory functions. Cell 136, 215–233.
Berensztein, E.B., Baquedano, M.S., Pepe, C.M., Mariana, C., Saraco, N.I., Roberto, P., Rivarola, M.A., Belgorosky, A., 2008. Role of IGFs and insulin in the human testis during postnatal activation: differentiation of steroidogenic cells. Pediatr. Res. 63, 662–666.
Bougneres, P., Goffin, V., 2007. The growth hormone receptor in growth. Endocrinol. Metab. Clin. North. Am. 36, 1–16.
Bubenik, G.A., Bubenik, A.B., Brown, G.M., Trenkle, A., Wilson, D.I., 1975. Growth hormone and cortisol levels in the annual cycle of white-tailed deer (*Odocoileus virginianus*). Can. J. Physiol. Pharmacol. 53, 787–792.
Butler, A., Le-Roith, D., 2001. Control of growth by the somatropic axis: growth hormone and the insulin-like growth factors have related and independent roles. Annu. Rev. Physiol. 63, 141–164.
Cao, H., Wang, L., Zhang, S., Lu, L., Sheng, X., Han, Y., Yuan, Z., Weng, Q., 2015. Seasonal expression of prolactin receptor in the scented gland of male muskrat (*Ondatra zibethicus*). Sci. Rep. 5, 15036.
Dantzer, B., Swanson, E.M., 2012. Mediation of vertebrate life histories via insulin-like growth factor-1. Biol. Rev. Camb. Philos. Soc. 87, 414–429.
Devesa, J., Almenglo, C., Devesa, P., 2016. Multiple Effects of Growth Hormone in the Body: Is it Really the Hormone for Growth? Clin. Med. Insights Endocrinol. Diabetes 9, 47–71.
Grishagin, I.V., 2015. Automatic cell counting with ImageJ. Anal. Biochem. 473, 63–65.
Gu, L., Mo, E., Yang, Z., Zhu, X., Fang, Z., Sun, B., Wang, C., Bao, J., Sung, C., 2007. Expression and localization of insulin-like growth factor-I in four parts of the red deer antler. Growth Factors 25, 264–279.
Han, W., Xie, W., Zhang, Y., Zhang, F., Zhang, H., Han, Y., Yuan, Z., Weng, Q., 2017. Seasonal expression of P450c17 and 5alpha-reductase-2 in the scented gland of male muskrats (*Ondatra zibethicus*). Gen. Comp. Endocrinol. 254, 60–67.
Harvey, S., 2010. Extrapituitary growth hormone. Endocrine 38, 335–359.
Harvey, S., Baudet, M.L., 2014. Extrapituitary growth hormone and growth? Gen. Comp. Endocrinol. 205, 55–61.
Harvey, S., Martinez-Moreno, C.G., Luna, M., Aramburo, C., 2015. Autocrine/paracrine roles of extrapituitary growth hormone and prolactin in health and disease: an overview. Gen. Comp. Endocrinol. 220, 103–111.
Hrabia, A., Paczoska-Eliasiewicz, H.E., Berghman, L.R., Harvey, S., Rzasa, J., 2008. Expression and localization of growth hormone and its receptors in the chicken ovary during sexual maturation. Cell Tissue Res. 332, 317–328.
Huang, H., Jiang, Y., Wang, Y., Chen, T., Yang, L., He, H., Lin, Z., Liu, T., Yang, T., Kamp, D.W., Wu, B., Liu, G., 2015. miR-5100 promotes tumor growth in lung cancer by

targeting Rab6. Cancer Lett. 362, 15–24.
Hull, K.L., Harvey, S., 2000. Growth hormone: roles in male reproduction. Endocrine 13, 243–250.
Hyun, S., 2013. Body size regulation and insulin-like growth factor signaling. Cell Mol. Life Sci. 70, 2351–2365.
Jing, J., Xiong, S., Li, Z., Wu, J., Zhou, L., Gui, J.F., Mei, J., 2015. A feedback regulatory loop involving p53/miR-200 and growth hormone endocrine axis controls embryo size of zebrafish. Sci. Rep. 5, 15906.
Kaiser, G.G., Sinowatz, F., Palma, G.A., 2001. Effects of growth hormone on female reproductive organs. Anat. Histol. Embryol. 30, 265–271.
Kamran, F., Andrade, A.C., Nella, A.A., Clokie, S.J., Rezvani, G., Nilsson, O., Baron, J., Lui, J.C., 2015. Evidence that up-regulation of MicroRNA-29 contributes to postnatal body growth deceleration. Mol. Endocrinol. 29, 921–932.
Kleinberg, D.L., Ruan, W., 2008. IGF-I, GH, and sex steroid effects in normal mammary gland development. J. Mammary Gland Biol. Neoplasia 13, 353–360.
Leroith, D., Werner, H., Beitner-Johnson, D., Roberts Jr., C.T., 2008. Molecular and cellular aspects of the insulin-like growth factor I receptor. Endocr. Rev. 16, 143–163.
Li, Q., Weng, J., Zhang, H., Lu, L., Ma, X., Wang, Q., Cao, H., Liu, S., Xu, M., Weng, Q., Watanabe, G., Taya, K., 2011. Immunohistochemical evidence: testicular and scented glandular androgen synthesis in muskrats (*Ondatra zibethicus*) during the breeding season. Eur. J. Histochem. 55, e32.
Lu, L., Liu, S., Li, Q., Huang, S., Bao, L., Sheng, X., Han, Y., Watanabe, G., Taya, K., Weng, Q., 2014. Seasonal expression of androgen receptor in scented gland of muskrat (*Ondatra zibethicus*). Gen. Comp. Endocrinol. 204, 1–7.
Lu, L., Zhang, H., Lv, N., Ma, X., Tian, L., Hu, X., Liu, S., Xu, M., Weng, Q., Watanabe, G., Taya, K., 2011. Immunolocalization of androgen receptor, aromatase cytochrome P450, estrogen receptor alpha and estrogen receptor beta proteins during the breeding season in scent glands of muskrats (*Ondatra zibethicus*). Zoolog. Sci. 28, 727–732.
Lui, J.C., 2017. Regulation of body growth by microRNAs. Mol. Cell. Endocrinol. 456, 2–8.
Lupu, F., Terwilliger, J.D., Lee, K., Segre, G.V., Efstratiadis, A., 2001. Roles of growth hormone and insulin-like growth factor 1 in mouse postnatal growth. Dev. Biol. 229, 141–162.
Nakamura, E., Otsuka, F., Inagaki, K., Miyoshi, T., Matsumoto, Y., Ogura, K., Tsukamoto, N., Takeda, M., Makino, H., 2012. Mutual regulation of growth hormone and bone morphogenetic protein system in steroidogenesis by rat granulosa cells. Endocrinology 153, 469–480.
Pitetti, J.L., Calvel, P., Zimmermann, C., Conne, B., Papaioannou, M.D., Aubry, F., Cederroth, C.R., Urner, F., Fumel, B., Crausaz, M., Docquier, M., Herrera, P.L., Pralong, F., Germond, M., Guillou, F., Jégou, B., Nef, S., 2013. An essential role for insulin and IGF1 receptors in regulating sertoli cell proliferation, testis size, and FSH action in mice. Mol. Endocrinol. 27, 814–827.
Ptak, A., Kajta, M., Gregoraszczuk, E.L., 2004. Effect of growth hormone and insulin-like growth factor-I on spontaneous apoptosis in cultured luteal cells collected from early, mature, and regressing porcine corpora lutea. Anim. Reprod. Sci. 80, 267–279.
Sanders, E.J., Harvey, S., 2004. Growth hormone as an early embryonic growth and differentiation factor. Anat. Embryol. (Berl) 209, 1–9.
Shenoy, A., Blelloch, R.H., 2014. Regulation of microRNA function in somatic stem cell proliferation and differentiation. Nat. Rev. Mol. Cell Biol. 15, 565–576.
Silberstein, G.B., 2015. Postnatal mammary gland morphogenesis. Microsc. Res. Technol. 52, 155–162.
Sirotkin, A.V., Mertin, D., Süvegová, K., Makarevich, A.V., Mikulová, E., 2003. Effect of GH and IGF-I treatment on reproduction, growth, and plasma hormone concentrations in domestic nutria (*Myocastor coypus*). Gen. Comp. Endocrinol. 131, 296–301.
Sjogren, K., Liu, J.L., Blad, K., Skrtic, S., Vidal, O., Wallenius, V., LeRoith, D., Tornell, J., Isaksson, O.G., Jansson, J.O., Ohlsson, C., 1999. Liver-derived insulin-like growth factor I (IGF-I) is the principal source of IGF-I in blood but is not required for postnatal body growth in mice. Proc. Natl. Acad. Sci. U.S.A. 96, 7088–7092.
Villalpando, I., López-Olmos, V., 2003. Insulin-like growth factor I (IGF-I) regulates endocrine activity of the embryonic testis in the mouse. J. Steroid. Biochem. Mol. Biol. 86, 151–158.
Villalpando, I., Lira, E., Medina, G., Garcia-Garcia, E., Echeverria, O., 2008. Insulin-like growth factor 1 is expressed in mouse developing testis and regulates somatic cell proliferation. Exp. Biol. Med. (Maywood) 233, 419–426.
Wagener, A., Blottner, S., Göritz, F., Fickel, J., 2000. Detection of growth factors in the testis of roe deer (*Capreolus capreolus*). Anim. Reprod. Sci. 64, 65–75.
Wang, J., Wang, Y., Zhu, M., Zhang, F., Sheng, X., Zhang, H., Han, Y., Yuan, Z., Weng, Q., 2017. Seasonal expression of luteinizing hormone receptor and follicle stimulating hormone receptor in testes of the wild ground squirrels (*Citellus dauricus* Brandt). Acta Histochem. 119, 727–732.
Woelfle, J., Billiard, J., Rotwein, P., 2003. Acute control of insulin-like growth factor-I gene transcription by growth hormone through Stat5b. J. Biol. Chem. 278, 22696–22702.
Xie, W., Liu, H., Liu, Q., Gao, Q., Gao, F., Han, Y., Yuan, Z., Zhang, H., Weng, Q., 2019. Seasonal expressions of prolactin, prolactin receptor and STAT5 in the scented glands of the male muskrats (*Ondatra zibethicus*). Eur. J. Histochem. 63, 2991.
Yagci, A., Zik, B., 2006. Immunohistochemical localization of insulin-like growth factor-I receptor (IGF-IR) in the developing and mature rat testes. Anat. Histol. Embryol. 35, 305–309.
Yoon, M., Berger, T., Roser, J.F., 2011. Localization of insulin-like growth factor-I (IGF-I) and IGF-I receptor (IGF-IR) in equine testes. Reprod. Domest. Anim. 46, 221–228.
Zhang, F., Liu, Q., Wang, Z., Xie, W., Sheng, X., Zhang, H., Yuan, Z., Han, Y., Weng, Q., 2017a. Seasonal expression of oxytocin and oxytocin receptor in the scented gland of male muskrat (*Ondatra zibethicus*). Sci. Rep. 7, 16627.
Zhang, H., Lu, L., Zhu, M., Zhang, F., Sheng, X., Yuan, Z., Han, Y., Watanabe, G., Taya, K., Weng, Q., 2017b. Seasonal expression of P450arom and estrogen receptors in scented glands of muskrats (*Ondatra zibethicus*). Am. J. Physiol. Regul. Integr. Comp. Physiol. 312, 380–387.
Zhang, H., Zhang, F., Zhu, M., Wang, J., Sheng, X., Yuan, Z., Han, Y., Watanabe, G., Taya, K., Weng, Q., 2017c. Seasonal expressions of follicle-stimulating hormone receptor and luteinizing hormone receptor in the scented gland of the male muskrat (*Ondatra zibethicus*). Am. J. Physiol. Regul. Integr. Comp. Physiol. 312, 569–574.
Zhang, T., Peng, D., Qi, L., Li, W., Fan, M., Shen, J., Yang, L., Wang, Y., Wang, W., Hu, X., Cai, R., Zhou, R., Wei, Y., Zhou, J., Yang, S., Hu, D., Liu, S., 2017d. Musk gland seasonal development and musk secretion are regulated by the testis in muskrat (*Ondatra zibethicus*). Biol. Res. 50, 10.